

Understanding the Catalytic Behavior of Zeolites: A First-Principles Study of the Adsorption of Methanol

Rajiv Shah; M. C. Payne; M.-H. Lee; Julian D. Gale

Science, New Series, Vol. 271, No. 5254 (Mar. 8, 1996), 1395-1397.

Stable URL:

http://links.jstor.org/sici?sici=0036-8075%2819960308%293%3A271%3A5254%3C1395%3AUTCBOZ%3E2.0.CO%3B2-S

Science is currently published by American Association for the Advancement of Science.

Your use of the JSTOR archive indicates your acceptance of JSTOR's Terms and Conditions of Use, available at http://www.jstor.org/about/terms.html. JSTOR's Terms and Conditions of Use provides, in part, that unless you have obtained prior permission, you may not download an entire issue of a journal or multiple copies of articles, and you may use content in the JSTOR archive only for your personal, non-commercial use.

Please contact the publisher regarding any further use of this work. Publisher contact information may be obtained at http://www.jstor.org/journals/aaas.html.

Each copy of any part of a JSTOR transmission must contain the same copyright notice that appears on the screen or printed page of such transmission.

JSTOR is an independent not-for-profit organization dedicated to creating and preserving a digital archive of scholarly journals. For more information regarding JSTOR, please contact support@jstor.org.

concerned the motion of sparse vortices. In the initial state, $T > T_c = 9.2 \text{ K}$ and B = 0.00After cooling the sample film below T_c , we applied B = 80 G and observed the vortices entering the film from its edges. These sparse vortices flowed on average in the direction perpendicular to the sample edges; hence, they were driven by the gradient in the vortex density, although individual vortices often hopped in scattered directions. The effect of the gradient in film thickness was appreciable only in the case of gentle vortex flows such as flux creep. The vortex hoppings were not completely independent from each other because a vortex hopping was often triggered by an approaching vortex. In the cases where a vortex was trapped in a defect (Fig. 5), the ensuing vortices would typically make detours to avoid the defect. Only rarely did collisions occur; sometimes an oncoming vortex recoiled after collision, and sometimes an oncoming vortex was trapped for a few seconds, followed by a release of a single vortex. These observations showed that the state of two vortices trapped in one defect should be unstable, as expected. No such correlations were found in the direction orthogonal to the direction of motion.

The second experiment concerned the case in which vortices are closely packed to form lattice domains. We applied B=180 G to the sample at $T>T_{\rm c}$, cooled the sample to T=4.5 K to find the latticedomain formation, and then reduced B to 85 G. After the lattice domains relaxed, the sample temperature was gradually raised to let the lattice domains move freely; they then exhibited more complicated and seemingly irreproducible motion in some cases.

A typical example is shown in Fig. 6. Just before the vortex flow began, the vortices formed lattice domains at 6 K (Fig. 6A). The domain size depended on experimental conditions; it was typically a few micrometers in diameter and contained 5 × 5 vortices. Each domain appeared to be pinned by the defects (Fig. 6A). The vortices remained stationary for a while, then suddenly began moving in "rivers" like avalanches near some domain boundaries (Fig. 6B). When vortices flowed in rivers, they became disordered. With an exposure time of 1/30 s (Fig. 6B), those vortices that moved were blurred and could only be seen as a river. The appearance of the river changed a little after 0.16 s (Fig. 6C). When the flow stopped, a new configuration of vortex lattices emerged (Fig. 6D), and domain boundaries were formed at different locations, which in turn triggered new avalanches. The duration of the flow depended on conditions but was generally <1 s. The velocity of a vortex hopping was on the order of 1 μ m s⁻¹.

The rivers flowed along the domain boundaries that were located near the defects; the vortex river in Fig. 6B emerged along the domain boundary located near the upper middle defect in Fig. 6A. At higher temperatures, the rivers became wider until the whole vortex lattice started to flow, keeping its form unchanged. These observations indicate that we visually monitored the transition from plastic to elastic flow.

REFERENCES AND NOTES

1. P. W. Anderson, Phys. Rev. Lett. 9, 309 (1962). 2. G. J. Van Gurp, Phys. Rev. 166, 436 (1968)

- 3. G. Blatter et al., Rev. Mod. Phys. 66, 1125 (1994).
- 4. S. Field et al., Phys. Rev. Lett. 74, 1206 (1995).
- 5. U. Yaron et al., Nature 376, 753 (1995)
- 6. K. Harada et al., ibid. 360, 51 (1992).
- 7. A. Tonomura, Electron Holography (Springer, Heidelberg, 1993).
- 8. A video clip is available at Science's Beyond the Printed Page site on the World Wide Web: http:// www.aaas.org/science/beyond.htm>.
- 9. We thank H. Hirose for assistance in irradiating an ion beam to Nb samples and H. Ezawa, C. N. Yang, and Y. S. Ono for valuable discussions and com-
 - 30 August 1995; accepted 12 December 1995

Understanding the Catalytic Behavior of Zeolites: A First-Principles Study of the Adsorption of Methanol

Rajiv Shah,* M. C. Payne, M.-H. Lee, Julian D. Gale

Zeolites are microporous aluminosilicate materials used as industrial catalysts, and there is much interest in understanding their catalytic behavior. The adsorption of methanol in the catalytically active zeolite chabazite and in sodalite was examined by performing ab initio calculations within periodic boundary conditions. A direct correlation between zeolite structure and chemical activation of the adsorbate was found. Methanol was protonated without an activation energy by a Brønsted acid site, provided the molecule was situated in the eight-ring window of chabazite, whereas the same molecule was only physisorbed in more open cage regions, such as those found in sodalite.

Microporous materials are powerful industrial catalysts, combining acidity with shape selectivity for reactants, products, and their intervening transition states (1). Amongst the wealth of chemical reactions catalyzed by these materials, one of the most important is the conversion of methanol, initially to dimethyl ether and subsequently to gasoline (2). Many experimental studies have characterized intermediate species of this reaction in situ (3), but we can still only speculate about the true mechanism. Methanol is known from infrared spectroscopy (4) to be initially adsorbed at acid sites in the zeolite framework, but the interpretation of such data in terms of either physisorbed methanol or chemisorbed methoxonium species (Fig. 1) is still a matter for debate (5).

There has been much interest in the use of quantum mechanical methods to determine the energetics of proton transfer from the zeolite framework to methanol, because this is believed to be the first step in the activation of the adsorbate. Most of these studies have used cluster methods, in which a small fragment of the zeolite is extracted and dangling bonds are saturated with hydrogen. By using a variety of ab initio techniques, it has been shown that methanol is

R. Shah, M. C. Payne, M.-H. Lee, Cavendish Laboratory (TCM), Madingley Road, Cambridge CB3 0HE, UK. J. D. Gale, Department of Chemistry, Imperial College, South Kensington SW7 2AY, UK

physisorbed and that the methoxonium ion is unstable, representing a transition state for the exchange of hydrogen between two oxygens (6, 7). However, most of these calculations represent only the local bonding interaction and neglect the long-range electrostatic potential, which could have a considerable effect given the partially ionic nature of aluminosilicates. Furthermore, such cluster models are often not specific to any one zeolite structure, and therefore the results cannot explain the different catalytic activities observed with varying framework topologies.

Recent advances in massively parallel computing, coupled with improved algorithms (8), have greatly increased the scope of first-principles quantum mechanical calculations for periodic systems, allowing investigation of the mechanism of zeolite catalysis. We have used such techniques to address the question of methanol adsorp-

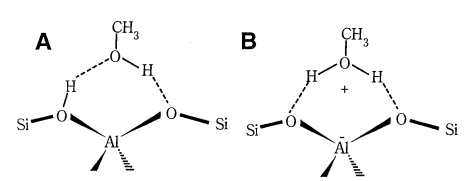


Fig. 1. Schematic illustration of the two possible adsorption complexes of methanol at an acid site (A) physisorbed with no proton transfer and (B) chemisorbed with proton transferred to form a methoxonium cation.

^{*}To whom correspondence should be addressed

tion, in order to avoid the uncertainty associated with the choice of cluster model and to allow us to examine differences in behavior associated with particular zeolite structures. We have used density functional theory (9) with a generalized gradient approximation (10) for the exchange-correlation energy and a plane-wave basis set to represent the wave functions (11). Structures were fully optimized at constant cell volume (12). The valence electrons were treated explicitly, with the nuclei and core electrons represented by pseudopotentials (13). The accuracy of the method was verified through the reproduction of the lattice parameter of α quartz, as well as the bond lengths and proton affinity of methanol in the gas phase [calculated value, -774 k] mol⁻¹; experimental value, -778 kJ mol⁻¹ (14)].

The main commercial catalyst for methanol conversion, ZSM-5, has a unit cell that is too large for accurate calculations to be performed with current computational resources. Instead, we have considered the chabazite structure (15), also known to be an active catalyst for the formation of dimethyl ether (16) but with a smaller unit cell of 12 tetrahedral sites and 24 framework oxygen atoms per unit cell. The periodicity imposed in the calculation results in a minimum loading of one methanol molecule per unit cell, giving an intermolecular separation of 9.2 Å. The interaction between molecules in neighboring unit cells was found in our calculations to be weak.

Experimentally, chabazite contains aluminum in about a third of all tetrahedral sites. However, we have chosen to consider a system with a Si/Al ratio of 11, that is, one aluminum atom per unit cell, to simplify the problem, because the number of possible conformations increases rapidly as the concentration of aluminum increases.

As a first step we determined the relative stability of the Brønsted acid sites formed by substitution of aluminum for silicon on a tetrahedral site, with protonation of an adjacent oxygen to maintain charge neutrality. There is one unique tetrahedral site in the asymmetric unit and therefore only four possible configurations, depending on which oxygen is protonated. All four acid sites were found to be stable local minima lying within an energy range of 15 kJ mol⁻¹. This is substantially greater than thermal energies under ambient conditions, suggesting that most of the protons will be located at the most stable oxygen, O3, assuming the hydrogen positions are determined thermodynamically rather than kinetically. At the temperatures used for performing zeolite catalysis, however, more sites may be accessible.

Previous cluster calculations (6) have demonstrated that physisorbed methanol

Table 1. Comparison between the geometry of methanol adsorbed in chabazite and free methanol or methoxonium. O(m), oxygen in the methanol molecule; O(f), oxygen in the zeolite framework. The bonds of the OH_2 group are about 10% longer than for the unadsorbed methoxonium and methanol. This is probably due to very strong hydrogen bonding, which is shown by the comparatively short distances between the hydrogens and the framework oxygens. Estimated accuracy $\pm 0.01\,\mathrm{\mathring{A}}$ (distances) and $\pm 0.5^\circ$ (angles).

Parameter	Adsorbed complex	Free methoxonium	Free methanol
Average C-H distance (Å)	1.09	1.09	1.10
C-O(m) distance (Å)	1.45	1.52	1.44
O(m)-H distance (Å)	1.04, 1.06	0.98, 0.98	0.97
O(f)-H distance (Å)	1.54, 1.38	_	-
H–O(m)–H angle	95.5°	108.8°	_
O(f)-H-O(m) angle	153.1°, 153.2°	_	_

forms a strong hydrogen bond with the acidic hydrogen of the framework; a second, weaker hydrogen bond is formed between the hydrogen of the methanol OH group and another oxygen bonded to aluminum. This scheme results in the formation of a six-membered ring structure (Fig. 1). Because there are six edges to the tetrahedral unit, each with two possible sites for proton binding, there are potentially 12 possible physisorbed geometries for methanol. However, many of these can be excluded because of steric hindrance. Here we consider the binding of methanol between O3 and

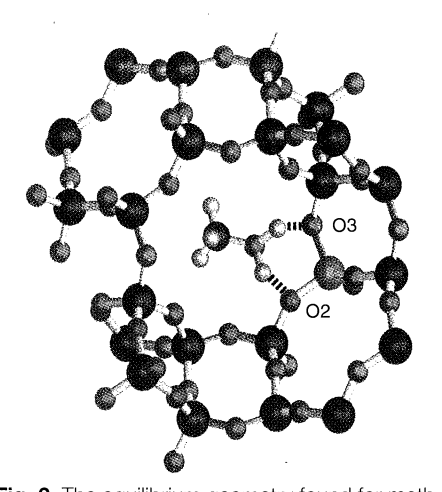


Fig. 2. The equilibrium geometry found for methanol adsorbed in chabazite. Gray atoms, Si; purple, Al; red, O; green, C; and blue, H. Dashed lines show hydrogen bonding. The molecule lies in the eight-ring window. The proton has been transferred to the methanol forming an OH_2 group, and the hydrogen atoms of this group are coordinated with framework oxygens adjacent to the Al site. Strong hydrogen bonding stabilizes the protonated complex. Two of the methyl hydrogens are between 2.8 and 3.1 Å from two or more framework oxygens on the far side of the window; the third is 3.8 Å from a framework oxygen.

O2, with the molecule situated in the eightring channel of the structure.

Starting with the proton coordinated to either O2 or O3, we found the same optimized geometry, that of a chemisorbed methoxonium ion (Fig. 2). There seems to be little or no barrier to proton transfer from the framework to methanol, given that we could not find a local minimum corresponding to a physisorbed complex. Haase and Sauer (7) have estimated from cluster calculations that the methoxonium ion is 12 kJ mol⁻¹ less stable than the physisorbed complex. In our periodic calculations, the electrostatic potential within the eight-ring appears to be sufficiently large to overcome this energy cost and allow charge separation to occur during the formation of an ion-pair structure.

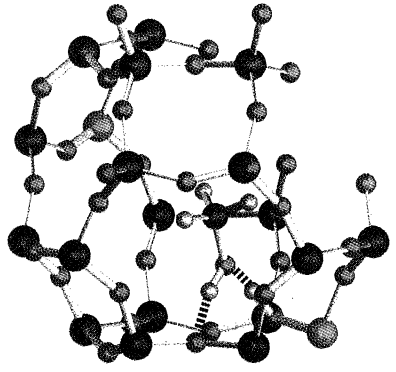


Fig. 3. The equilibrium geometry found for methanol adsorbed in sodalite. Atom colors and dashed lines are as in Fig. 2. The proton remains bound to the zeolite framework, and the methanol lies in the cage region of the framework. The methanol hydrogen bridges across to the oxygen on the other side of the six-ring rather than simply across the aluminum. One methyl hydrogen is 3.0 Å from a framework oxygen; the others are >3.5 Å from any of the framework oxygens.

The geometry of the adsorbed complex was compared to that of the free species (Table 1). The methoxonium cation forms two strong hydrogen bonds, with nonbonded O-H distances as short as 1.35 Å. This value agrees with the trend observed in cluster calculations, in which the hydrogen bond length decreases as the size of the model increases; values as low as 1.41 Å have been observed for large systems. This finding is consistent with the behavior observed in $H_5O_2^+$, in which the proton almost symmetrically bridges between two water molecules with distances of close to 1.2 Å (17). The particularly strong hydrogen bonding also explains the large hydroxyl stretching frequency shifts observed in the infrared spectrum (4). Our calculated heat of adsorption for methanol, 82 kJ mol^{-1} , is within the large range of experimental estimates (63 to 120 kJ mol^{-1}) measured for various zeolites (7, 18).

For comparison, we also examined the adsorption of methanol at an acid site in a highly siliceous form of the sodalite structure, again with a Si/Al ratio of 11. Although sodalite has the same number of atoms per unit cell as chabazite, the structure is very different, made up of β cages linked to give a small channel aperture, consisting of six-rings rather than the eight-rings found in chabazite. This structure does not have pores into which methanol could penetrate, and the acidic form is experimentally not known, but the sodalite cage is a unit found in several more complex structures such as zeolite A.

Steric hindrance prevents methanol from lying in the six-ring windows, and thus the molecule is situated in the more open cage region of the structure. We found that methanol was physisorbed instead of chemisorbed, with the proton remaining bound to the zeolite framework (Fig. 3). Despite the different structures of the adsorption complexes in the two structures, the binding energy of methanol in sodalite was similar to that in chabazite (73 kJ mol^{-1}).

We conclude that there is a delicate balance between the physisorbed and chemisorbed states of methanol in aluminosilicates. The nature of the adsorption complex is crucially dependent on the structure of the zeolite being considered. Contrary to previous cluster calculations (6, 7), calculations taking into account the full periodicity of the zeolite structure show instances in which proton transfer from the zeolite to methanol takes place. In regions containing medium-sized pores, it appears that methanol is preferentially adsorbed and is activated through protonation. In the case of chabazite this process occurs in the eight-ring window, and we can infer from the catalytic activity of ZSM-5 that the same is probably true for 10-rings. When methanol is situated in the more open cage regions of zeolites, it appears to be unprotonated and potentially less chemically active.

We speculate that the medium-sized pores are the most active site for methanol reaction, because these are where methanol appears to be protonated. The presence of both methanol and methoxonium species in regions with different structural characteristics may explain the difficulty in unambiguously assigning experimental infrared spectra. We have demonstrated the potential of periodic ab initio calculations to treat molecular adsorption in aluminosilicates, which can now be extended to aid the elucidation of the reaction pathways of methanol within such heterogeneous catalysts.

Note added in proof: Our results for the case of adsorption of methanol in sodalite are consistent with recently published calculations of infrared spectra (19).

REFERENCES AND NOTES

- 1. J. M. Thomas, Philos. Trans. R. Soc. London Ser. A 333, 173 (1990).
- 2. S. L. Meisel, J. P. McCullogh, C. H. Lechthaler, P. B. Weisz, Chem. Technol. 6, 86 (1976).
- 3. M. W. Anderson and J. Klinowski, Nature 339, 200
- 4. G. Mirth, J. A. Lercher, M. W. Anderson, J. Klinowski, J. Chem. Soc. Faraday Trans. **86**, 3039 (1990).
- 5. G. Mirth and J. A. Lercher, in Natural Gas Conversion, A. Holmen et al., Eds. (Elsevier, Amsterdam, 1991), pp. 437-443.
- 6. J. D. Gale, C. R. A. Catlow, J. R. Carruthers, Chem. Phys. Lett. 216, 155 (1993).
- 7. F. Haase and J. Sauer, *J. Am. Chem. Soc.* **117**, 3780

- 8. M. C. Payne, M. P. Teter, D. C. Allan, T. A. Arias, J. D. Joannopoulos, Rev. Mod. Phys. 64, 1045 (1992).
- 9. P. Hohenberg and W. Kohn, Phys. Rev. 136, B864 (1964); W. Kohn and L. J. Sham, ibid. 140, A1133 (1965).
- 10. The Perdew-Wang functional was used [J. P. Perdew, in Flectronic Structure of Solids '91 P Zeische and H Eschrig, Eds. (Akademie Verlag, Berlin, 1991).
- 11. A plane wave cutoff of 650 eV was used, and Brillouin zone sampling was performed only at the $\boldsymbol{\Gamma}$ point. We estimate the error due to these approximations to be about 2 kJ mol-1
- 12. Ab initio norm-conserving pseudopotentials were used. Those for carbon and oxygen were kinetic energy-optimized by Qc filter tuning [M. H. Lee et al., in preparation.
- 13. Optimization was performed with no symmetry constraints, until forces were <0.03 eV/Å. The estimated error in energy of relaxed structure was <2 kJ
- 14. D. H. Aue and M. T. Bowers, in Gas Phase Ion Chemistry, M. T. Bowers, Ed. (Academic Press, New York, 1979), vol. 2, p. 18.
- 15. L. S. Dent and J. V. Smith, Nature 181, 1794 (1958).
- G. P. Tsintskaladze, A. R. Nefedova, Z. V. Gryaznova, G. V. Tsitsishvili, M. K. Charkviani, Zh. Fiz. Khim. 58, 718 (1984).
- 17. Y. Xie, R. B. Remington, H. F. Schaefer III, J. Chem. Phys. 101, 4878 (1994).
- 18. U. Messow, K. Quitzsch, H. Herden, Zeolites 4, 255
- 19. E. Nusterer, P. E. Blöchl, K. Schwarz, Angew. Chem. 35 (no. 2), 175 (1996).
- This work was performed on the Cray T3D at Edinburgh Parallel Computing Centre as part of the United Kingdom Cas-Parinello and Materials Chemistry consortia. R.S. acknowledges the Engineering and Physical Sciences Research Council for financial support and J.D.G. thanks the Royal Society for provision of a University Research Fellowship.

27 October 1995; accepted 16 January 1996

Reversible Cleavage and Formation of the Dioxygen O-O Bond Within a Dicopper Complex

Jason A. Halfen, Samiran Mahapatra, Elizabeth C. Wilkinson, Susan Kaderli, Victor G. Young Jr., Lawrence Que Jr., Andreas D. Zuberbühler, William B. Tolman*

A key step in dioxygen evolution during photosynthesis is the oxidative generation of the O–O bond from water by a manganese cluster consisting of M₂(μ–O)₂ units (where M is manganese). The reverse reaction, reductive cleavage of the dioxygen O-O bond, is performed at a variety of dicopper and di-iron active sites in enzymes that catalyze important organic oxidations. Both processes can be envisioned to involve the interconversion of dimetal-dioxygen adducts, $M_2(O_2)$, and isomers having $M_2(\mu-O)_2$ cores. The viability of this notion has been demonstrated by the identification of an equilibrium between synthetic complexes having $[Cu_2(\mu-\eta^2:\eta^2-O_2)]^{2+}$ and $[Cu_2(\mu-O)_2]^{2+}$ cores through kinetic, spectroscopic, and crystallographic studies.

Dioxygen O-O bond-forming and bondcleaving reactions occur at transition metal centers in a number of enzymes. For example, O-O bond cleavage occurs at mononu-

J. A. Halfen, S. Mahapatra, E. C. Wilkinson, V. G. Young Jr., L. Que Jr., W. B. Tolman, Department of Chemistry, University of Minnesota, Minneapolis, MN 55455, USA. S. Kaderli and A. D. Zuberbühler, Institute of Inorganic Chemistry, University of Basel, CH-4056 Basel, Switzerland.

*To whom correspondence should be addressed.

clear heme (cytochrome P-450) (1) and nonheme di-iron (methane monooxygenase) (2-4) centers that hydroxylate alkanes to produce key metabolites. Similar reactions are needed for the oxidation of tyrosine by a dicopper active site to form L-dopa (tyrosinase) (5) and by a nonheme di-iron center to generate the catalytically essential radical of ribonucleotide reductase (3, 4, 6). The reverse reaction, the oxidative coupling of water molecules to form O₂